Modelling and Control of a nonlinear distillation column: A, using fractional-order controllers

Omar Hanif
Department of Automatic Control and Systems Engineering
The University of Sheffield
Sheffield, United Kingdom
omar.hanif@ieee.org

Shipra Tiwari
Department of Electrical Engineering
Motilal Nehru National Institute of Technology
Prayagraj, India
tiwarishipra80@gmail.com

Vivek Kumar
Department of Electrical Engineering
Indian Institue of Technology Roorkee
Roorkee, Uttarakhand,
India
Vivek_k1@ee.iitr.ac.in

2021 IEEE 18th India Council International Conference (INDICON) | 978-1-6654-4175-9/21/$31.00 ©2021 IEEE | DOI: 10.1109/INDICON52576.2021.9691748

***Abstract*—This paper takes up the challenge of modelling a complex nonlinear distillation column type-A and designs four optimal controllers for the same. The nonlinear plant is first linearized into a linear higher-order model. Thereafter, it is reduced into a lower-order model. Subsequently, the controllers are designed for the lower-order linear model. The controllers are designed by reducing the error cost functions, namely Integral Square Error (ISE), Integral Absolute Error (IAE) and Integral Time Absolute Error (ITAE). The process of optimization is done heuristically using the Genetic Algorithm method of tuning. The four controllers designed are Proportional Integral Derivative, Fractional-order Proportional Integral Derivative, Tilt Integral Derivative and Fractional-order Internal Model Control. A thorough comparison is made between the three designed controllers, first on the Single Input Single Output (SISO), then to the reduced-order linear model and finally to the main plant. The FO-IMC controller is shown as an exhibition controller designed using GA to demonstrate the novelty of its kind. It has also been compared, but the results show poor performances as it has not been tuned with the same parameters as the rest.**

Keywords—Nonlinear System Identification, Fractional-Order PID (FOPID), Tilt-Integral Derivative, Fractional-order Internal Model Control, Genetic Algorithm.

I. INTRODUCTION

A. Background of Fractional-order control

The earliest publications on FOPID controller and fractional-order system (FOS) were carried out by I. Podlubny in 1994. The main focus of I. Podlubny was mainly on an applied controller of FOPID and FOS. After the research, he concluded that fractional-order compared to the FOPID showed positive responses and to be more flexible to tune than the integer-based counterpart. An optimal FOPID controller was designed based upon reducing the Integral Absolute Error as a cost function. It became the most remarkable and initial works done on the FOPID [1]. In 1994 Lurie et al. constructed a novel type of fractional-order, termed Tilt-Integral-Derivative (TID). I. Podlubny also demonstrated the study Mittag-Leffler function in 1999 and transformation of Laplace to study the dynamics of Fractional-order system (FOS) in different domains of time. D. Xue et al. (2002) did a comprehensive work on the FOCs. The robust nature of the fractional-order controllers is also highlighted in the paper [2]. The stability of the fractional-order system is similar to the integer-order counterpart. Both of the systems included asymptotic stability and BIBO (bounded-input-bounded-output) [3].

B. Advantage of FOCs over PID Controllers

The Fractional-order Controller (FOCs) are meant to be better than classical PID in the following ways:
(a) FOC performed better in terms of reference tracking (servo response).
(b) They are better than classical PID in rejecting disturbances (disturbance is fed in the distillation column).
(c) They anticipate the uncertainties and hence provide better robustness.
(d) They provide a high margin of stabilities, i.e. Gain Margin and Phase Margin compared with PID.
(e) They cater better noise rejection in the system.
(f) When applied to the nonlinear system, they provide better-desired results [4].

II. BASIC CONCEPTS

A. Construction and Working of a Distillation column

The distillation column is considered to be a power demanding procedure. The working is based on separating two or more materials in the components' desired purity by removing the heat from the components. Mostly the separation is based upon the boiling points and the relative volatility. The least volatile substance is known as heavy compounds; on the other hand, the most volatile components are known as light substances. The control aspect of the distillation column would be desired concentration level of the distillate product (Y_d Kmol/min), the desired concentration level of the bottom product (X_d Kmol/min), desired level of the distillate product (M_d Kmol) and desired level of the bottom product (M_b). The various inputs are Reflux (L), Boil up the flow (V), Distillate Flow (D), Bottom Flow (B), Feedrate (F), Mole Fraction (z_F).

B. Fractional Order Controllers

Some of the famous FOCs are FOPID, TID and FO-IMC controller (written in order) in (1) and (2)

$$C(s) = K_p + \frac{k_i}{s^\lambda} + k_d s^\mu \;\; ; \;\; C(s) = \frac{k_t}{s^{\frac{-1}{n}}} + \frac{k_i}{s} + k_d s \qquad (1)$$

$$C(s) = \frac{1}{(s^p + a)}\left(K_p + \frac{k_i}{s^\lambda} + k_d s^\mu\right) \qquad (2)$$

The above equation (1) and (2) represent the controller transfer function of FOPID, TID and FO-IMC controller, which is similar to a PID controller except for a fractional power $s^{-\lambda}, s^{\mu}, s^{\frac{-1}{n}}$. Similarly, FO-IMC has the same structure as that of FOPID with only the difference of fractional-order filter 'p' and constant 'a', whose ranges $p\epsilon[1,2]$ and a could take any small integer value.

FOC's have higher degrees of freedom where λ, μ and n ($n\epsilon[2,3]$) can take infinite values following the desired output to be obtained [4]. Figure 1 shows the area in which the controllers FOPID and PID can work, shown along with their

978-1-6654-4175-9/21/$31.00 ©2021 IEEE

Authorized licensed use limited to: INDIAN INSTITUTE OF TECHNOLOGY ROORKEE. Downloaded on February 08,2023 at 13:26:22 UTC from IEEE Xplore. Restrictions apply.

ranges. The values of parameters taken by PID are only three, and $area_{PID} = 0$. However, FOPID could take infinite values of the tuning parameter [5].

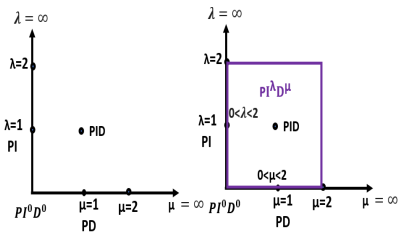

FIGURE 1: TUNING AREA OF PID (LEFT) AND FOPID (RIGHT PURPLE)

C. Nonlinear Systems

Nonlinear system does not observe the principle of homogeneity and superposition, (3) and (4) show the nonlinear system's general equation.

$$x(t) = f(x(t), u(t), t) \quad (3)$$

$$y(t) = f(x(t), u(t), t) \quad (4)$$

From above, it is observed that the 'y' represents the output and x (t) represents the state vector shows $\in R^n$, u(t) represents the input vector $\in R^N$ and y(t) is output vector $\in R^q$.

C.1. Points of Equilibrium

The point of equilibrium is represented where the nonlinear function $f(x_e)=0$. In a control system, the equilibrium points are shown as $f(x_e,u_e)=0$. The points of equilibrium help to obtain linearized version of the nonlinear model. Taylor's series formula of linearization shown in (5).

$$F(x(t), u(t), t) = f(x0, u0) + \partial f \partial t[x(t), u(t), t]|x0(x(t) - x0) + \partial f \partial t[x(t), u(t), t]|u0(u(t) - u0) + H.O.T \quad (5)$$

C.2. Multi-input Multi-output system

A system that takes 'n' number of inputs to give 'p' number of outputs is called the MIMO system. The characteristic of the MIMO system is that the inputs and outputs affect each other even if they are not meant to be directly related. This gives another term Relative Gain Array (RGA), which decides the correct dependence of respective inputs to outputs. The inputs of MIMO systems are considered to be MVs (manipulated variables) or DVs (disturbance variables).

III. METHODOLOGY

The methodology is represented in the flowchart in figure 2.

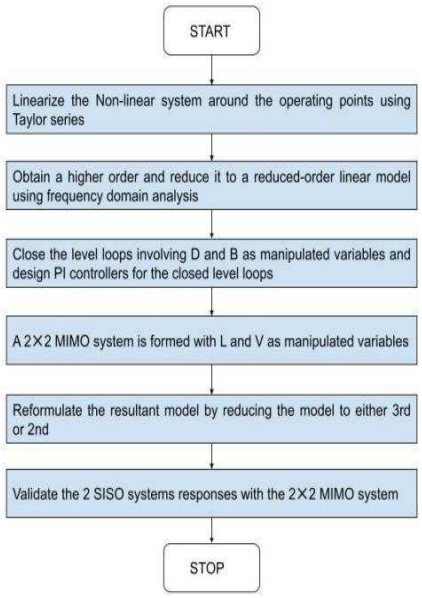

FIGURE 2: DEVELOPMENT OF A MODEL OF DISTILLATION COLUMN A

IV. CONTROL

The control algorithm is represented in the flowchart in figure 3.

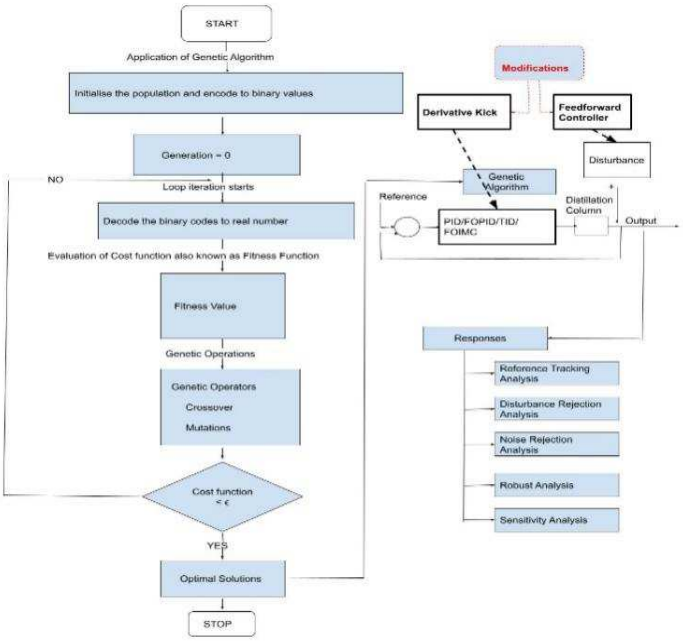

FIGURE 3: THE CONTROL DESIGN METHODOLOGY

V. RESULTS

The results could be divided into *A* Modelling/system identification results *B.* Control results.

A. System Identification Results

The model taken is Skogested Distillation column Type-A [6]. The following steps are performed. *Step1.* The operating points around which the model is linearized is also given in [6] in the table named Nominal operating values of the

Authorized licensed use limited to: INDIAN INSTITUTE OF TECHNOLOGY ROORKEE. Downloaded on February 08,2023 at 13:26:22 UTC from IEEE Xplore. Restrictions apply.

distillation column. The resultant linear model is of 82nd order. This 82nd order linear model is reduced using the Henkel method of model-order reduction into 8th order model. The open-loop responses of the actual nonlinear system with that of linear 82nd order and 8th order is compared in figure 4.

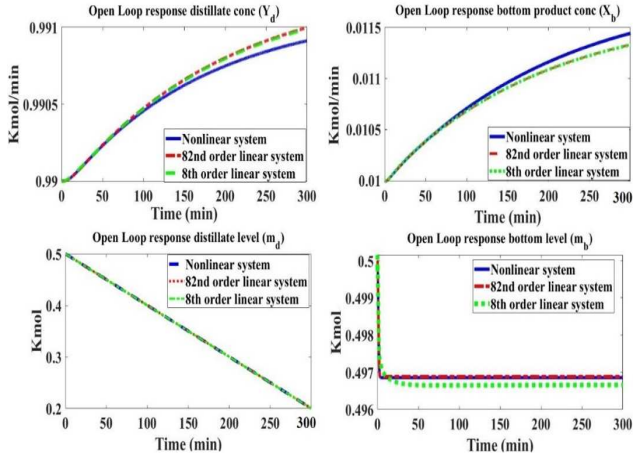

FIGURE 4: OPEN-LOOP RESPONSES VALIDATION OF 8TH ORDER AND 82ND ORDER WITH ACTUAL NONLINEAR PLANT

The comparison of the nonlinear and open models shows a satisfactory result with a simulated time of 300 minutes. *Step2.* Since there are four inputs (L, V, D, B) and two disturbance inputs (F and z_F) [6] followed by four outputs, the next thing is to close some of the loops and design a controller for it. For it, the level loop is closed first, and the PI controllers are designed.

The online method (Zeigler-Nichols) is employed to tune the controllers of PI. In order to get a better response, the parameters are adjusted manually [7]. In (6) and (7), the formulated PI controllers are shown.

$$C_1 = -0.827 + 0.551s \tag{6}$$

$$C_2 = -2.175 + 1.450s \tag{7}$$

The calculation of the static RGA for the 8th order linear system to study the interaction between the loops is in (8).

$$\Lambda = \begin{matrix} & U_1 & U_2 \\ L & 0.9571 & 0.0429 \\ V & 0.0429 & 0.9571 \end{matrix} \tag{8}$$

From the RGA, the most used pairs are u_2(V) with y_2(X_b) with u_1(L) with y_1(Y_d). *Step3.* Construction of decouplers in order to reduce the interaction between the loops. The responses of two matrix states after closing the level-loops in *Step2.* is shown in (9).

$$\begin{bmatrix} L \\ Y \end{bmatrix} = \begin{bmatrix} \frac{8.1\times10^{-5}s^3+0.004s^2}{s^3+0.005s^2-4.07\times10^{-27}s} & \frac{-3.2\times10^{-5}s^3+0.005s^2}{s^3+0.005s^2+1.310\times10^{-27}s} \\ \frac{+2\times10^{-17}s-3.65\times10^{-33}}{-1.03\times10^{-50}} & \frac{+2\times10^{-17}s+4\times10^{-33}}{+8.032\times10^{-36}} \\ \frac{8.5\times10^{-5}s^3-0.004s^2}{s^3+0.005s^2-4.79\times10^{-25}s} & \frac{-0.00014s^3-0.0058s^2}{s^3+0.005s^2+1.401\times10^{-27}s} \\ \frac{-1.96\times10^{-17}s+8.4\times10^{-34}}{+8.82\times10^{-49}} & \frac{-2.77\times10^{-17}s-9.08\times10^{-34}}{+8.5\times10^{-36}} \end{bmatrix} \begin{bmatrix} Y_d \\ X_b \end{bmatrix} \tag{9}$$

Equation (10) is used for designing decoupler. Figure 7 shows the decoupler.

$$G_{dec1} = G_{12}G_{22}\ ;\ G_{dec2} = G_{21}G_{11}\ ; \tag{10}$$

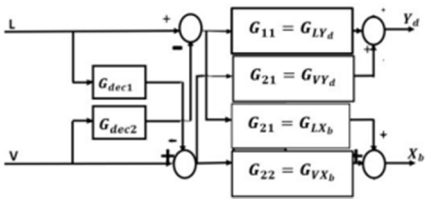

FIGURE 7: PERFECT- DECOUPLERS FOR THE MIMO SYSTEM

$$G_{dec1} = \frac{3.25\times10^{-5}s^6 - 0.0055s^5 - 2.97\times10^{-5}s^4 + 1.687\times10^{-19}s^3 + 9.52\times10^{-35}s^2 - 8.06\times10^{-62}s - 3.45\times10^{-87}}{0.000149s^6 + 0.0058s^5 + 2.96\times10^{-5}s^4 - 1.394\times10^{-19}s^3 - 5.18\times10^{-35}s^2 - 9.60\times10^{-61}s - 3.76\times10^{-87}} \tag{11}$$

$$G_{dec2} = \frac{8.5\times10^{-5}s^6 - 0.004s^5 - 2.21\times10^{-5}s^4 + 4.48\times10^{-20}s^3 + 4.05\times10^{-36}s^2 - 1.27\times10^{-57}s - 9.01\times10^{-81}}{8.15\times10^{-5}s^6 + 0.0044s^5 + 2.29\times10^{-5}s^4 - 5.12\times10^{-20}s^3 - 9.83\times10^{-36}s^2 - 5.5\times10^{-60}s - 2.9\times10^{-82}} \tag{12}$$

The application of decoupler is shown, and the MIMO system of 2x2 is converted into two SISO loops system such as:

$$Y_d = (V - LG_{dec1})G_{21} + (L - VG_{dec2})G_{11} \tag{13}$$

$$Y_d = VG_{21} - LG_{21}G_{dec1} + LG_{11} - VG_{dec2}G_{11} \tag{14}$$

From (13) and (14), the values L and V are taken as common.

$$Y_d = L(G_{11} - G_{21}G_{12}G_{22}) = L(G_{11} - G_{21}G_{dec1}) \Leftrightarrow \boldsymbol{Y_d = LG_{SISO1}} \tag{15}$$

Similarly, for the other loop X_b

$$X_b = (V - LG_{dec1})G_{22} + (L - VG_{dec2})G_{12} \tag{16}$$

$$X_b = VG_{22} - LG_{22}G_{dec1} + LG_{12} - VG_{dec2}G_{12} \tag{17}$$

$$X_b = V(G_{22} - G_{12}\tfrac{G21}{G11}) = VG_{22} - VG_{dec2}G_{12} \Leftrightarrow \boldsymbol{X_b = VG_{SISO2}} \tag{18}$$

The decouplers are an important part of a MIMO system. They decentralize the system into two SISO loops, as shown in figure 8.

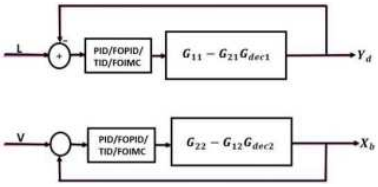

FIGURE 8: TWO SISO LOOPS AFTER DECENTRALIZATION

Step2. Validation is very important for any system's modelling. Figure 9 shows the validation of the responses of two-SISO loops with the 8th order linear MIMO loop for distillate concentration Y_d and bottom concentration X_b. They are almost overlapping, which means that the perfect decoupler without disturbance (no F and z_F) is approximately matched to the 8th-order linear MIMO model.

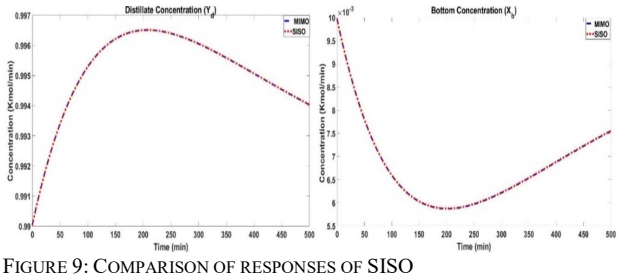

FIGURE 9: COMPARISON OF RESPONSES OF SISO

Authorized licensed use limited to: INDIAN INSTITUTE OF TECHNOLOGY ROORKEE. Downloaded on February 08,2023 at 13:26:22 UTC from IEEE Xplore. Restrictions apply.

B. Control Results

Let $\rho = \varphi = \gamma = 0.5$, are the weights. The cost functions involve reference tracking error, and disturbance rejection error is J_1 and J_2. Hence the total cost function is J_{total} is the minimization of both errors.

$$J_1 = \rho \int_0^\infty \mathrm{t}|e_r|\mathrm{dt} + \varphi \int_0^\infty {e_r}^2\mathrm{dt} + \gamma \int_0^\infty |e_r|\mathrm{dt} \quad (19)$$

$$J_2 = \rho \int_0^\infty \mathrm{t}|e_2|\mathrm{dt} + \varphi \int_0^\infty {e_d}^2\mathrm{dt} + \gamma \int_0^\infty |e_d|\mathrm{dt} \quad (20)$$

$$J_{total} = J_1 + J_2 \quad (21)$$

The controller so obtained is an improper transfer function. Therefore, a filter is added to make their proper function. The filter function taken is $\frac{1}{(1000s+1)}$. The controllers so obtained are written in Table I. They are analysed and compared on *(1). Reference tracking and controller's effort (2). Regulatory responses (3). Noise rejections (4). Robustness (5). Application on the 8th-order MIMO and real nonlinear distillation column system*.

TABLE I. OPTIMAL PID AND ITS FRACTIONAL-ORDER VARIANTS

SISO plant 1		SISO plant 2
G1(s) = $\frac{6.29\times10^{-5}s^2+0.01178s^2+0.01687s+3.67\times10^{-6}}{s^3+39.2s^2+0.3934s+0.0009845}$		**G2(s) =** $\frac{-0.00011s^3-0.021s^2-0.030s-6.57\times10^{-6}}{s^3+54.99s^2+0.5683s+0.001468}$
PID	$199.23 + \frac{197.21}{s} + 0.02s$	$-199.95 - \frac{197.71}{s} - 39.33s$
TID	$\frac{198.23}{\frac{-1}{s^{2.89}}} + \frac{197.21}{s} + 0.06s$	$\frac{-199.92}{\frac{-1}{s^{2.02}}} - \frac{199.95}{s} - 0.018s$
FOPID	$195.94 + \frac{197.21}{s^{0.611}} + 199.80s^{0.552}$	$-199.93 - \frac{199.98}{s^{0.6363}} - 154.06s^{0.503}$
FO-IMC	$\frac{1}{(s^{1.921}+0.00212)}(2.20 + \frac{0.5047}{s^{1.035}} + 496s^{1.19})$	$\frac{1}{(s^{1.2095}+0.0022)}(-1.42 - \frac{1.5047}{s^{5.61}} - 295.2s^{1.13})$

B.1. Servo Responses and Controllers' effort:

The reference tracking of the three controllers on the 2 SISO plants is shown in figure 10. The response characteristics, i.e., rise time, settling time, total controller's effort (TV), Integral Square Error (ISE), Integral Absolute Error (IAE) and Integral Time Absolute Error (ITAE), are tabulated in Table II.

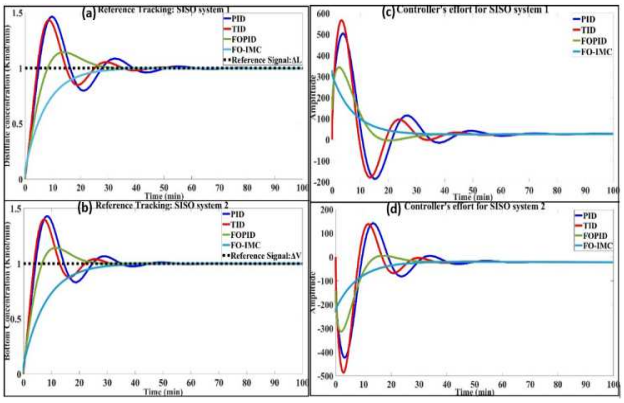

FIGURE 10: (A), (B) REFERENCE TRACKING (C),(D) CONTROLLER'S EFFORT

TABLE II. COMPARISON OF CONTROLLERS BASED ON SERVO RESPONSE AND CONTROLLER'S EFFORT

SISO system: 1 (simulation time = 200 minutes)							
Controller	T_r	T_S	M_p	**TV**	**ISE**	**IAE**	**ITAE**
PID	3.9	47.7	46.5	2.1×10^4	0.018	0.017	0.022
TID	3.5	33.5	43.2	2.6×10^4	0.017	0.018	0.017
FOPID	6.3	27.5	14.8	1.1×10^4	0.016	0.0168	0.013
FO-IMC	17	29.2	0.001	1.0×10^4	0.019	0.019	0.025
SISO system: 2 (simulation time = 200 minutes)							
Controller	T_r	T_S	M_p	**TV**	**ISE**	**IAE**	**ITAE**
PID	3.5	41.4	42.9	1.6×10^4	0.166	0.19	0.183
TID	3.1	32.8	39.8	1.9×10^4	0.163	0.19	0.131
FOPID	5.2	23.1	14.5	1.5×10^4	0.161	0.18	0.103
FO-IMC	18	28.3	7.5×10^{-4}	8.1×10^4	0.168	0.19	0.187

Observations: Figure 10 and Table II show that the TID controller exhibits the fastest rise time for both plants. The reason for this is, a small integrator at the proportional gain side ($K_t/s^{-0.35}$) causing the faster response. The FOPID controller shows a faster rise time to the classical PID and the fastest settling time for both plants. The conventional PID shows a high peak overshoot as compared to its fractional-order hybrids. The FO-IMC has the slowest rise time but considerably faster settling time. Finally, the errors in ISE, IAE and ITAE of each fractional-order controller are lesser than classical PID. The FO-IMC shows considerably more error since the tuning parameters are taken are not the same as the rest of the controllers. It is just shown as an exhibition exercise for tuning FO-IMC using GA (which proves the novel design of FO-IMC).

B.2. Disturbance Rejection

The reduction of error is the prime motive of the distillation column A control. The SISO plants are subjected to the disturbances: Feed rate (F) and composition effects (z_F) at the 10th minute. The controllers' responses for the disturbance rejection are shown in figure 11 and tabulated in Table III.

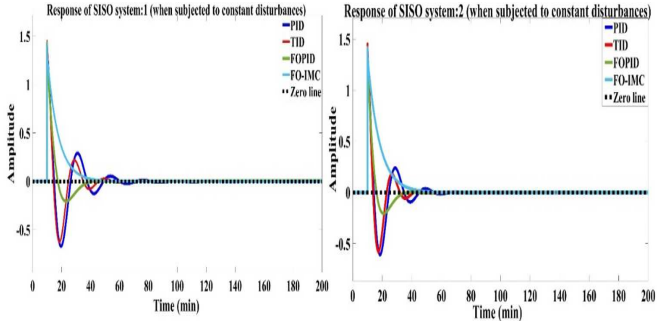

FIGURE 11: COMPARISON OF CONTROLLERS

TABLE III. COMPARISON OF CONTROLLER BASED ON DISTURBANCE REJECTIONS

Authorized licensed use limited to: INDIAN INSTITUTE OF TECHNOLOGY ROORKEE. Downloaded on February 08,2023 at 13:26:22 UTC from IEEE Xplore. Restrictions apply.

SISO system: 1 (simulation time = 200 minutes)					
Controllers	T_r	T_S	*ISE*	*IAE*	ITAE
PID	1.09×10^{-9}	51.78	0.059	0.15	1.53
TID	3.58×10^{-10}	38.81	0.056	0.132	1.32
FOPID	1.03×10^{-15}	32.18	0.055	0.125	1.37
FO-IMC	12.4×10^{-6}	41.29	0.069	0.15	1.63
SISO system: 2 (simulation time = 200 minutes)					
Controllers	T_r	T_S	*ISE*	*IAE*	ITAE
PID	1.83×10^{-10}	57.40	0.065	0.143	1.57
TID	3.61×10^{-11}	43.46	0.063	0.139	1.49
FOPID	1.03×10^{-12}	36.48	0.058	0.136	1.42
FO-IMC	1.45×10^{-5}	39.16	0.070	0.153	1.62

The FOPID shows the fastest response for the disturbance rejection, followed by the TID controller. Also, the disturbance rejection error is least for the fractional-order hybrids of the PID controller. This implies that the fractional-order controllers are better in rejecting the unwanted federate and the feed compositions [9,10]. The FO-IMC shows considerably more error since the tuning parameters are taken are not the same as the rest of the controllers. It is just shown as an exhibition exercise for tuning FO-IMC using GA (which proves the novel design of FO-IMC).

B.3. Noise Rejection:

A noisy signal of SNR 20.5 dB is introduced at the sensor end of both the SISO loops and the rejection responses are shown in figure 12 and tabulated in Table IV.

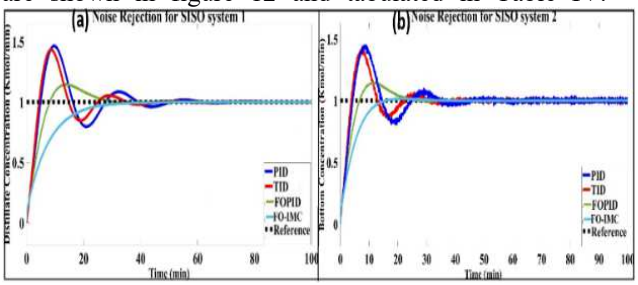

FIGURE 12: (A) AND (B) COMPARISON OF CONTROLLERS ON NOISE REJECTIONS FOR THE TWO LOOPS

TABLE IV. COMPARISON OF CONTROLLER BASED ON NOISE REJECTIONS

Controllers	SISO system 1 Total Variation (simulation time = 100mins)	SISO system 2 Total Variation (simulation time = 100mins)
PID	1.339×10^{-5}	1.171×10^{-4}
TID	1.413×10^{-5}	1.571×10^{-4}
FOPID	5.212×10^{-6}	7.921×10^{-5}
FO-IMC	9.411×10^{-7}	8.478×10^{-6}

From Fig 8 and Table IV, it can be inferred that FO-IMC is the best attenuator of the rest of the controllers (though it's not compared rigorously in the paper). FOPID also proves to be better than PID. PID shows better results than TID; the reason lies in the small integrand of the TID controller at the proportional gain end [11].

B.4. Relative Stability Analysis:

The controller should provide stability to the plant. Hence, relative stability becomes a crucial parameter for comparing the controllers for indicating the more the stable system is (plant + controller). The frequency response for both the SISO plants with the controller are shown in figure 13, and the margins of stability are tabulated in Table V.

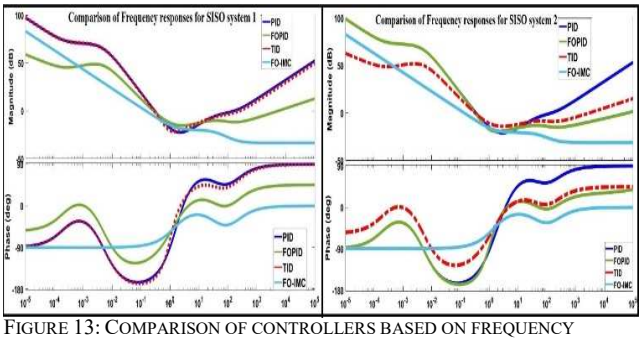

FIGURE 13: COMPARISON OF CONTROLLERS BASED ON FREQUENCY RESPONSES

TABLE V. COMPARISON OF CONTROLLER BASED ON STABILITY MARGINS

Stability margins for controllers of the SISO system: 1		
Controllers	**Gain Margin (dB)**	**Phase Margin (degrees)**
PID	Very High	29.1
TID	Very High	32.1
FOPID	Very High	72.8
FO-IMC	Very High	95.6
Stability margins for controllers of the SISO system: 2		
PID	24.2	34.4
TID	26.6	26.4
FOPID	15.2	73.8
FO-IMC	Very High	95.2

The Gain Margin (GM) of all the controllers concerning the SISO system 1 shows a very high value. A theoretical analysis of the Distillation column A. Although, FO-IMC shows most stability in GM for SISO system 2. The Phase Margin (PM) of both SISO systems 1 and 2 for the fractional-order controllers are better than the classical PID.

B.5. Robust Analysis:

The controllers are compared by simulating four different uncertainties, and their GM and PM are tabulated in Table VI for both of the SISO plants.

TABLE VI. ROBUST ANALYSIS

Robust analysis on controllers for SISO plant 1					
Cont/ original values	**Gain increased 50%**	**Gain increased 100%**	**Time delay added**	**Dominant Pole added**	**Faster Pole added**
PID Pm=30.2 at 0.303rad/s	Change % = 20.53 Pm=36.4° at 0.378 rad/s	Change % = 36.63 Pm=47° at 0.492 rad/s	Change % = 28.15 Pm=21.7° at 0.305 rad/s	Change % = 56.29 Pm=13.2° at 0.296 rad/s	Change % = 113.91 Pm=64.6° at 0.0078 rad/s
TID Pm=22.9 at 0.284rad/s	Change % = 23.14 Pm=28.2° at 0.346 rad/s	Change % = 44.1 Pm=33° at 0.399 rad/s	Change % = 34.93 Pm=14.9° at 0.286 rad/s	Change % = 69.83 Pm=6.91° at 0.284 rad/s	Change % = 118.75 Pm=57.5° at 0.0093 rad/s
FOPID Pm=72.1 at 0.263rad/s	Change % = 11.37 Pm=80.3° at 0.356 rad/s	Change % = 21.91 Pm=87.9° at 0.45 rad/s	Change % = 10.26 Pm=64.7° at 0.264 rad/s	Change % = 20.8 Pm=57.1° at 0.257 rad/s	Change % = 20.31 Pm=49.24° at 0.0353 rad/s

Authorized licensed use limited to: INDIAN INSTITUTE OF TECHNOLOGY ROORKEE. Downloaded on February 08,2023 at 13:26:22 UTC from IEEE Xplore. Restrictions apply.

FO-IMC Pm=95.6 at 0.145rad /s	Change % = 2.93 Pm=98.4° at 0.219 rad/s	Change % = 5.65 Pm=101 ° at 0.295 rad/s	Change % = 28.66 Pm=68.2° at 22.8 rad/s	Change % = 8.68 Pm=87. 3° at 0.144 rad/s	Change % = 5.86 Pm=90° at 0.0002 rad/s
Robust analysis on controllers for SISO plant 2					
Cont/ original values	**Gain increased 50%**	**Gain increas ed 100%**	**Time delay added**	**Domin ant Pole added**	**Faster Pole added**
PID Pm=30.2 at 0.303rad /s	Change % = 20.53 Pm=36.4° at 0.378 rad/s	Change % = 36.63 Pm=47 ° at 0.492 rad/s	Change % = 28.15 Pm=21.7° at 0.305 rad/s	Change % = 56.29 Pm=13. 2° at 0.296 rad/s	Change % = 113.91 Pm=64. 6° at 0.0078 rad/s
TID Pm=22.9 at 0.284rad /s	Change % = 23.14 Pm=28.2° at 0.346 rad/s	Change % = 44.1 Pm=33 ° at 0.399 rad/s	Change % = 34.93 Pm=14.9° at 0.286 rad/s	Change % = 69.83 Pm=6.9 1° at 0.284 rad/s	Change % = 118.75 Pm=57. 5° at 0.0093 rad/s
FOPID Pm=72.1 at 0.263rad /s	Change % = 11.37 Pm=80.3° at 0.356 rad/s	Change % = 21.91 Pm=87. 9° at 0.45 rad/s	Change % = 10.26 Pm=64.7° at 0.264 rad/s	Change % = 20.8 Pm=57. 1° at 0.257 rad/s	Change % = 20.31 Pm=49. 24° at 0.0353 rad/s
FO-IMC Pm=95.6 at 0.145rad /s	Change % = 2.93 Pm=98.4° at 0.219 rad/s	Change % = 5.65 Pm=10 1° at 0.295 rad/s	Change % = 28.66 Pm=68.2° at 22.8 rad/s	Change % = 8.68 Pm=87. 3° at 0.144 rad/s	Change % = 5.86 Pm=90 ° at 0.0002 rad/s

A thorough, robust analysis is covered in Table VI. The 'change %' refers to the change in stability margins when the SISO plant is introduced to uncertainties. The PM is only recorded since the GM comes out to infinity since it is a theoretical case study. As soon as the system's gain is increased, the PM and the crossover frequency are increased. Also, delay and the dominant pole addition decreases the PM. It can be inferred that the fractional-order controllers FO-IMC (novel controller) followed by FOPID show the least deviation to the uncertainties. The TID is least capable of providing robustness to the plant. The small integrand of the TID could be again accountable for its high oscillation and less robustness.

B.6. Application to the 8th-order MIMO plant:

After being analyzed thoroughly on the two SISO plants, the designed controllers are tested on the 8th order MIMO distillation column with perfect decouplers designed in the earlier section. The rate of reflux 'ΔL' (which is the input for the distillate concentration) is varied as a step pulse. Likewise, the rate of boil-up 'ΔV' is changed as step-pulse. The disturbances are also added, which are F and z_f . The latter are simulated at a low frequency with nominal amplitude of 1 and 0.5, respectively [12]. The responses for each of the four controllers are shown in figure 14 and tabulated in VII.

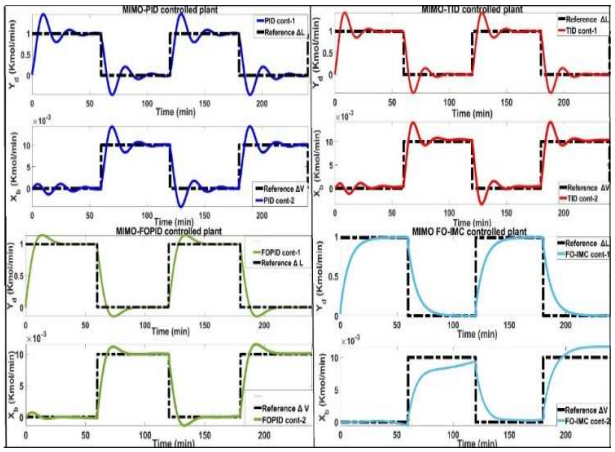

FIGURE 14 : COMPARISON OF PID AND ITS VARIANTS ON MIMO 8TH ORDER PLANT

TABLE VII. COMPARISON OF PID AND IT'S VARIANTS ON MIMO 8TH ORDER PLANT

Controllers	ISE	IAE
PID	1.3396 (Y_d) 2.6857×10^{-4} (X_b)	30.9136 (Y_d) 0.2584 (X_b)
TID	1.1440 (Y_d) 2.5715×10^{-4} (X_b)	32.2147 (Y_d) 0.2773 (X_b)
FOPID	0.0802 (Y_d) 4.5715×10^{-4} (X_b)	21.2312 (Y_d) 0.0931 (X_b)
FO-IMC	1.6877 (Y_d) 6.041×10^{-4} (X_b)	36.803 (Y_d) 0.266 (X_b)

The distillate concentration (Y_d) and bottom (X_b) respectively show the tracking of the setpoint change for all controllers. The FOPID controller proves to be better on the 8th-order linear MIMO plant with a perfect decoupler. It shows the least error even though a model mismatch (SISO model is an approximation). The FO-IMC shows considerably more error since the tuning parameters are taken are not the same as the rest of the controllers. It is just shown as an exhibition exercise for tuning FO-IMC using GA (which proves the novel design of FO-IMC).

B.7. Application on the Nonlinear plant:

The final purpose of the controllers build on the SISO plant is to test against the actual distillation column A plant. The responses of all the controllers for the distillate concentration (Y_d), bottom concentration (X_b), distillate level (M_d) and bottom level (M_b) are shown in figure 15 and tabulated in Table VIII.

Authorized licensed use limited to: INDIAN INSTITUTE OF TECHNOLOGY ROORKEE. Downloaded on February 08,2023 at 13:26:22 UTC from IEEE Xplore. Restrictions apply.

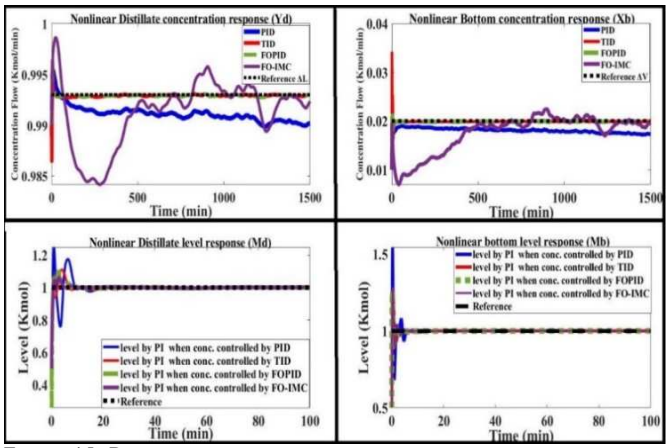

FIGURE 15: RESPONSE OF ALL CONTROLLERS

TABLE VIII. NONLINEAR PLANT RESPONSES

Nonlinear plant with Optimal Controllers				
Controllers	Y_d	X_b	M_d	M_b
PID	4.69×10^{-4}	4.20×10^{-4}	0.7265	0.2490
TID	1.26×10^{-4}	3.15×10^{-4}	0.3003	0.2716
FOPID	5.64×10^{-5}	7.26×10^{-5}	0.2031	0.2454
FO-IMC	0.0082	0.0135	0.1033	0.0920

The fractional-order controllers show better responses for all the desired outputs for the nonlinear distillation column A. Also, the error accountable for the fractional-order controller is minimum when compared with the classical PID controller.

VI. CONCLUSION

The fractional-order control presents a huge amount of flexibility in tuning the parameters, reaching the level, and getting pleasurable responses. A nonlinear distillation column type A with configuration of the LV control is taken as a case study. Detailed modeling of nonlinear distillation columns is presented in the early sections. The design of the control system is also discussed in the later sections. The controllers are designed by applying the genetic algorithm in optimizing the multiple cost functions of errors during tracking of reference and rejection of disturbances. These controllers are TID, FOPID, FO-IMC and PID. A thorough comparison is carried on these four controllers, firstly on the SISO systems, then on the linearized MIMO system and finally on the main plant. Overall the fractional-order controllers provide better responses as compared to their integer-order controllers.

REFERENCES

1. Podlubny, Igor. "Fractional-order systems and fractional-order controllers." Institute of Experimental Physics, Slovak Academy of Sciences, Kosice 12, no. 3 (1994): 1-18.
2. Xue, Dingyu, and YangQuan Chen. "A comparative introduction of four fractional order controllers." In Proceedings of the 4th World Congress on Intelligent Control and Automation (Cat. No. 02EX527), vol. 4, pp. 3228-3235. IEEE, 2002.
3. Petras, Ivo. "Stability of fractional-order systems with rational orders." arXiv preprint arXiv:0811.4102 (2008).
4. Sondhi, Swati, and Yogesh V. Hote. "Fractional order controller and its applications: a review." Proc. of AsiaMIC (2012).
5. Hammami, Rahma, Imène Ben Ameur, and Khaled Jelassi. "Asynchronous machine vector control: PIα controllers for current loops." Proceedings of the Institution of Mechanical Engineers, Part I: Journal of Systems and Control Engineering 234, no. 1 (2020): 107-117.
6. Skogestad, Sigurd. "Dynamics and control of distillation columns: A tutorial introduction." Chemical Engineering Research and Design 75, no. 6 (1997): 539-562.
7. Seborg, Dale E., Duncan A. Mellichamp, Thomas F. Edgar, and Francis J. Doyle III. Process dynamics and control. John Wiley & Sons, 2010.
8. Caponetto, Riccardo, and Emanuele Murgano. "Model Order Reduction: a comparison between Fractional and Integer Order Approximation." In 2019 IEEE International Conference on Systems, Man and Cybernetics (SMC), pp. 2037-2041. IEEE, 2019.
9. Caponetto, Riccardo, Juan J. Trujillo, and José A. Tenreiro Machado. "Theory and applications of fractional order systems 2016." (2016).
10. Monje, Concepción A., YangQuan Chen, Blas M. Vinagre, Dingyu Xue, and Vicente Feliu-Batlle. Fractional-order systems and controls: fundamentals and applications. Springer Science & Business Media, 2010.
11. Luo, Ying, Yang Quan Chen, Chun Yang Wang, and You Guo Pi. "Tuning fractional order proportional integral controllers for fractional order systems." Journal of Process Control 20, no. 7 (2010): 823-831.
12. Haji, Vahab Haji, and Concepción A. Monje. "Fractional-order PID control of a MIMO distillation column process using improved bat algorithm." Soft Computing 23, no. 18 (2019): 8887-8906.

Authorized licensed use limited to: INDIAN INSTITUTE OF TECHNOLOGY ROORKEE. Downloaded on February 08,2023 at 13:26:22 UTC from IEEE Xplore. Restrictions apply.